Journal of Nuclear Materials 386–388 (2009) 919–921

Contents lists available at ScienceDirect

Journal of Nuclear Materials

journal homepage: www.elsevier.com/locate/jnucmat

Erosion simulation of first wall beryllium armour under ITER transient heat loads

B. Bazylev [a,*], G. Janeschitz [b], I. Landman [a], S. Pestchanyi [a], A. Loarte [c]

[a] Forschungszentrum Karlsruhe, IHM, P.O. Box 3640, 76021 Karlsruhe, Germany
[b] Forschungszentrum Karlsruhe, Fusion, P.O. Box 3640, 76021 Karlsruhe, Germany
[c] ITER Organisation, Cadarache, 13108 Saint Paul Lez Durance Cedex, France

ARTICLE INFO

PACS:
52.40Hf

ABSTRACT

The beryllium is foreseen as plasma facing armour for the first wall in the ITER in form of Be-clad blanket modules in macrobrush design with brush size about 8–10 cm. In ITER significant heat loads during transient events (TE) are expected at the main chamber wall that may leads to the essential damage of the Be armour. The main mechanisms of metallic target damage remain surface melting and melt motion erosion, which determines the lifetime of the plasma facing components. Melting thresholds and melt layer depth of the Be armour under transient loads are estimated for different temperatures of the bulk Be and different shapes of transient loads. The melt motion damages of Be macrobrush armour caused by the tangential friction force and the Lorentz force are analyzed for bulk Be and different sizes of Be-brushes. The damage of FW under radiative loads arising during mitigated disruptions is numerically simulated.

1. Introduction

So far, most of the modeling effort on damage to plasma facing components (PFC) under transient loads in ITER was concentrated upon the divertor target [1–6]. Namely, a significant effort has been recently dedicated to study and model the damage to the divertor W and CFC armour for the disruptions and Type I ELM loads [1–6]. It is foreseen that the beryllium PFC components will be located at the main chamber wall of ITER (Be-clad blanket modules in macrobrush design with brush size about 8–10 cm).Thus, it seems that a similar study for Be-clad armour is also necessary, because significant heat loads during transient events (TE) are expected at the main chamber wall [7]. The expected thermal fluxes Q at the **First wall (FW)** caused by the dumped plasma on the ITER PFCs during ITER transients are: Type I ELM: $Q = 0.5–2$ MJ/m^2, $\tau = 0.3–0.6$ ms. The thermal quench: $Q = 0.5–5$ MJ/m^2, $\tau = 1–3$ ms. The mitigated disruptions stimulated by massive noble gas injection into ITER vessel generate radiative loads at the FW $Q = 0.1–2$ MJ/m^2 and $\tau = 0.2–1.0$ ms. The intense radiative heat loads at the FW may also be caused by the tungsten or carbon vapor expanded into SOL from the divertor region after the transient events.

The numerical simulations completed for the tungsten armours [1–6] demonstrated: In the ITER even for moderate and weak ELMs the main mechanisms of metallic armour damage remain the surface melting and melt motion erosions caused by the direct action of dumped plasma on the target surface as well as by the Lorentz force of the currents crossing the melt layer in the strong applied magnetic field. The simulations demonstrated also that armour macrobrush structure can prevent violent melt motion for the TE, which significantly decreases the final magnitude of melt erosion.

The aim of this work is to provide reliable estimations of the damage to the Be-clad blanket modules under the mentioned Type I ELM and the disruption thermal quench loads (using the code MEMOS [1–6]). The melting thresholds and melt layer depth of the Be armour under transient loads ($Q = 0.2–2$ MJ/m^2 and $\tau = 0.2–0.6$ ms) are estimated for different shapes of the transient. The results of numerical simulations) of the erosion due to evaporation are also presented. The melt motion damage of Be macrobrush armour caused by the tangential friction force is analyzed for different sizes of Be-brushes and compared with the bulk Be target. The damage of FW under radiative heat arising during mitigated disruptions is estimated. The radiative heat loads at the FW during these disruptions are calculated by the code FOREV and transferred into the code MEMOS as input data and further MEMOS simulations are carried out.

2. Numerical simulations of Be armour erosion

Bulk Be armour erosion: melting thresholds. The final Be armour damage significantly depends on heat load source: either dumped plasma or radiation heats the armour surface. In case of plasma impact ionized vapor shield protects the surface from the most intense impact of hot plasma. That leads to significant decreasing the erosion due to evaporation in comparison with the radiation action at the armour surface. In the last case shielding is negligible. The dependences of evaporation depths on the energy

* Corresponding author.
E-mail address: bazylev@ihm.fzk.de (B. Bazylev).

0022-3115/$ - see front matter © 2009 Elsevier B.V. All rights reserved.
doi:10.1016/j.jnucmat.2008.12.236

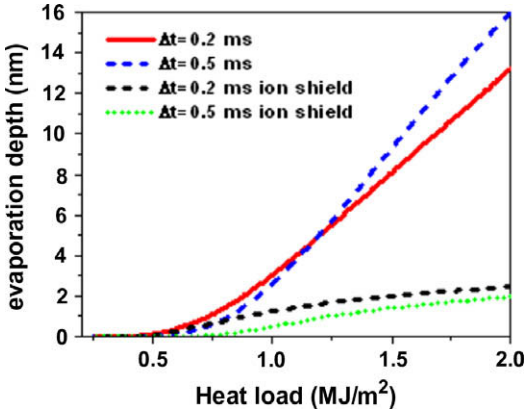

Fig. 1. Dependence of evaporation depth on the heat load.

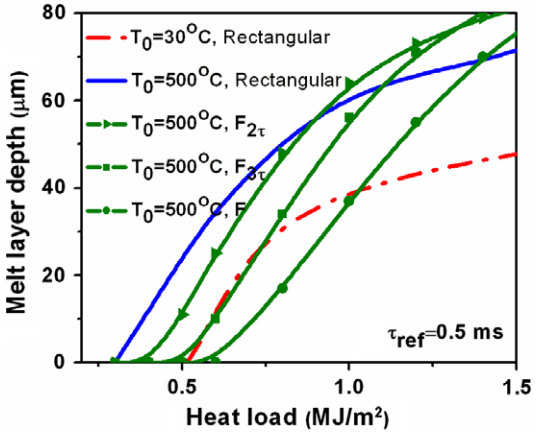

Fig. 3. Depth of melt pool as function of heat loads for different initial temperatures of the bulk Be and different pulse shapes.

heat load for $\tau = 0.2$ ms and $\tau = 0.5$ ms calculated by the code MEMOS are presented in Fig. 1. With the vapor shielding, maximum evaporated material thickness slightly exceed 2 μm whereas the radiation heat load leads to monotonic growth of evaporated material thickness.

The numerical simulations, carried out for the rectangular and "real" ELMs-like [8] (Eq.(1)) heat loads demonstrated that melting threshold and calculated melt layer thickness essentially depend on the temperature of the bulk target and the shape of the heat loads. For ELMs-like heat loads 3 type of the shape were chosen: the full pulse, the pulse cut off at $t = 2\tau$ and the pulse cut off at $t = 3\tau$ (Eqs. (1), Fig. 2).

$$Q(t) \propto F(t) = \left(1 + \left(\frac{\tau}{t}\right)^2\right)\left(\frac{\tau}{t}\right)^2 \exp\left(-\left(\frac{\tau}{t}\right)^2\right) \times \int_0^{\infty} F(t)\,dt \approx 1.2\tau, \quad \int_0^{3\tau} F(t)\,dt \approx \tau, \quad \times \int_0^{2\tau} F(t)\,dt \approx \tau/1.2 \qquad (1)$$

For the "real pulse" the total heat load varies within 40% depending on pulse tail (see Eqs. (1)). Dependences of the melt pool depth as function of the heat load for the reference ELM with $\tau = 0.5$ ms are demonstrated in Fig. 3 for different bulk temperatures and heat load shapes. The melt layer depth is always below 80 μm. The "real" shape of TE leads to increasing the melting threshold up to factor 2 in comparison with the rectangular TE shape and decreasing the melt thickness up to factor 2 depending on the pulse tail. Thus magnitude of the allowed ITER ELMs may be increased at least by factor 1.5.

For other duration of TE (τ_d) the melt layer depth ($L(Q_d, \tau_d)$) can be roughly estimated in accordance with Eq. (2):

$$L(Q_d, \tau_d) = L_B(Q_d, 0.5)\sqrt{2\tau_d} \qquad (2)$$

where $L_B(Q_d, 0.5)$ is the melt thickness taken from Fig. 3 and τ_d in ms.

Be macrobrush armour erosion caused by the melt motion. Numerical simulations of Be armour damage caused by the plasma stream action were carried out for the Be bulk and macrobrush designed armour. The sizes of the macrobrush elements are the following: the diameter of brushes $D = 1$ cm, 2 cm, 4 cm, 8 cm, the width of the gaps between brushes 1 mm. The Be target is heated with the energy deposition of the Gaussian spatial profile with the half-width $H_w = 10$ cm and the plasma beam width 15 cm. Influences of the tangential friction force and the Lorentz force (as mostly important driving force [3–6]) on the Be-brush target damage are investigated: the tangential friction force was varied in the range $p_{||} = 0, -0.02$ bar and the Lorentz force in the range 0.1–2 kA/cm^2. The reference ELM heat load $Q = 1$ MJ/m^2 with $\tau = 0.5$ ms and rectangular shape are assumed. The tangential friction force generates violent melt motion with the velocities (V_{max}) exceeding 7 m/s at the bulk target, about 1.2 m/s at the Be-brush target with $D = 1$ cm and 5.5 m/s for $D = 4$ cm and about 7 m/s for $D = 8$ cm (see Fig. 4). Such violent melt motion leads to formation of the final

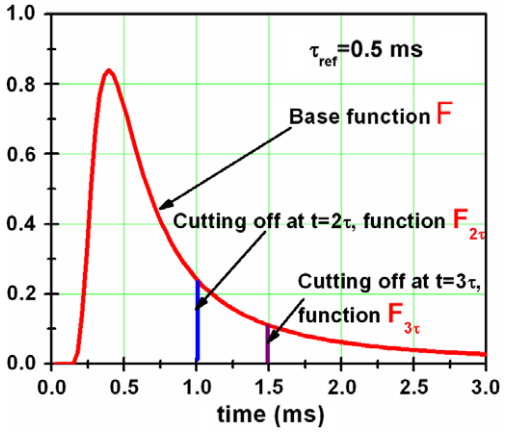

Fig. 2. Fundamenski "real" ELM-like heat load function with different methods of the tail cutoff.

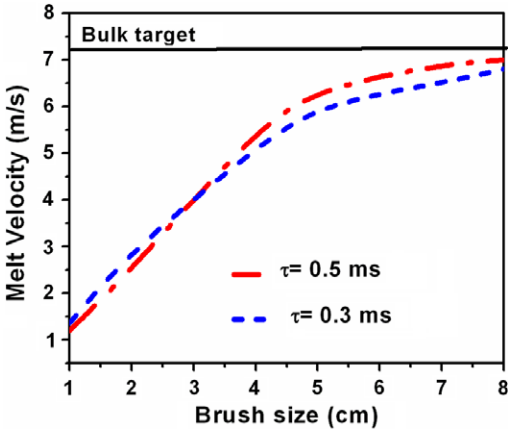

Fig. 4. Dependence of V_m as function of brush sizes. Reference ELMs with $Q = 1$ MJ/m^2, $\tau = 0.5$ ms and $\tau = 0.3$ ms, $p_{||} = 0.02$ bar.

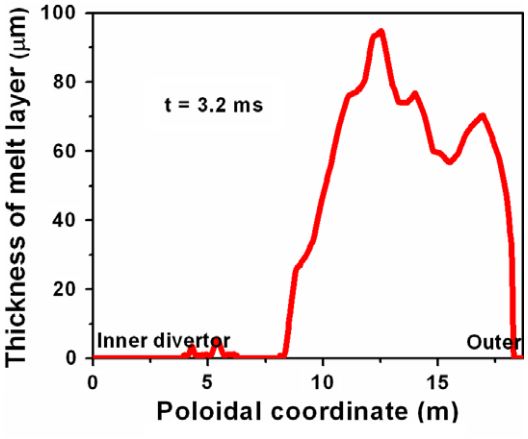

Fig. 5. Distribution of melt pool depth along poloidal coordinate.

roughness of 6 μm in case of the bulk Be target and about 1 μm at the brush edges for macrobrush target with $D = 1$ cm, and about 4 cm for $D = 2$ cm. The final brush roughness for cases $D < 2$ is less than 2 μm, whereas for the Be-brush target with $D > 4$ cm the final brush roughness is comparable with that of bulk Be armour.

Numerical simulations for reference ELM and magnetic field of 5 T demonstrated that the Lorentz force generates violent melt motion with the velocities exceeding 1.5 m/s for $I = 0.5$ kA/cm^2, 3.5 m/s for $I = 1$ kA/cm^2 and 7.5 m/s for $I = 2.0$ kA/cm^2. Such melt motion causes formation of the roughness of about ten micrometer per one ELM.

Be first wall damage under radiative heat load during mitigated disruptions. The scenarios of mitigated disruptions with the energy release of 30, 40, 60 and 130 MJ/ms of the plasma energy during 3 ms were simulated by the code FOREV to obtain the radiation fluxes at the FW. These fluxes are used as input data in the MEMOS simulations. Numerical simulation demonstrated that upper and outer walls are the mostly irradiated regions. The disruption scenarios, in which carbon plasma expands from the divertor with negligible penetration into the pedestal (30, 40, 60 MJ/ms), are not so dangerous for the FW. The maximum of the surface temperature does not reach the melting temperature remaining below 1100 K. In case of the higher energy release (130 MJ/ms) with penetration of the carbon plasma in the pedestal in considerable quantities radiation fluxes at the FW significantly increase practically along the entire FW. That leads to significant increasing the surface temperature above to 2000 K, melting Be armour along approximately 10 m after 1.5 ms. The depth of melt layer reaches 100 μm at the Upper wall that can be seen in Fig. 5. So high surface temperature of the Be armour leads to essential evaporation of Be in average of about 0.5 μm on distance about 5 m along the upper wall. Maximum evaporation depth reaches 1.7 μm.

3. Conclusion

The melting threshold and melt layer depth essentially depend on the TE shape. In case of the right ELM shape the threshold of the allowed ITER ELMs can be increased by factor 1.5.

Numerical simulation demonstrated that the velocity of melt motion and damage to the macrobrush targets with the sizes $D \leqslant 2$ cm is significantly (by factor 4) less in comparison with that of bulk Be.

The Lorentz force can generates violent melt motion that leads to the roughness formation exceeding 10 μm per one ELM.

Acknowledgements

This work, supported by the European Communities under the contract of Association between EURATOM and Forschungszentrum Karlsruhe, was carried out within the framework of the European Fusion Development Agreement. The views and opinions expressed herein do not necessarily reflect those of the European Commission.

References

[1] B. Bazylev, H. Wuerz, J. Nucl. Mater. 307–311 (2002) 69.
[2] B. Bazylev et al., Europhy-sics Conference Abstracts, vol. 27A, P-2.44.
[3] B. Bazylev et al., J. Nucl. Mater. 337–339 (2005) 766.
[4] B.N. Bazylev et al., Fusion Eng. Des. 75–79 (2005) 407.
[5] B.N. Bazylev et al., Phys. Scr. T128 (2007) 229.
[6] B.N. Bazylev et al., J. Nucl. Mater. 363–365 (2007) 1011.
[7] A. Loarte et al., in: Proceedings of the 21st IAEA Conference Chengdu, 16–21 October 2006. ISNB 92-0100907-0/ISSN 0074-1884.
[8] W. Fundamenski et al., Plasma Phys. Controlled Fusion 48 (2006) 109.